Efficiency of Organic Corrosion Inhibitors Derived from Thai-Bael Fruit Extract for Preventing Corrosion in Carbon Steels

Phattarasuda Manantapong[1], Nattanon Chaipunya[1], Suttipong Wannapaiboon[2], Prae Chirawatkul[2], Worawat Wattanathana[1] and Yuranan Hanlumyuang[1,*]

[1]Department of Materials Engineering, Faculty of Engineering, Kasetsart University, Ladyao, Chatuchak, Bangkok 10900, Thailand
[2]Synchrotron Light Research Institute, 111 University Avenue, Suranaree, Muang, Nakhon Ratchasima 30000, Thailand

*Corresponding author: E-mail: yuranan.h@ku.th

The inhibiting action of Thai-bael fruit extract at room temperature on hot-rolled steel in 1M HCl solution was studied. The chemical functional groups of the green inhibitors were characterized by Fourier-transformed infrared spectroscopy. The electrochemical activities of steel surface were investigated through linear polarization measurements, electrochemical impedance spectroscopy, surface assessment techniques based on optical microscopy and X-ray absorption spectroscopy. Electrochemical testing samples have been prepared in the form of square plates with the size 1×1 cm². The organic corrosion inhibitor extract from Thai-bael fruit has shown the smallest corrosion current density (I_{corr}) of 114.8 µA cm² and corrosion potential (E_{corr}) of -424.6 mV, compared with standard Ag/AgCl electrode potential. In comparison, similar tests in the bare HCl solutions yielded I_{corr} = 882.4 mA cm² and E_{corr} = -445.8 mV. The mixed-type corrosion inhibiting behaviour was evidenced in the results of the polarization measurements. Electrochemical impedance spectroscopy reveals that the resistance to charge transfer due to the presence of the extracts has been increased by about four times that of the same test on the bare HCl solution, indicating the formation of a protective layer. The adsorption of the organic molecules near the steel-electrolyte interface is evident in the decreasing double-layer capacitance with the enhancing concentration levels of the extract. This latter finding supports the displacement of the water molecules by means of the adsorption of the inhibitors on the steel surface. The optical images of steel surface before and after being immersed in HCl solution also showed pieces of evidence of corrosion retardation. XANES study as well as the linear combination fitting revealed that the samples immersed in HCl solutions with Thai-bael fruit extract possess less Fe^{3+} compositions. All tendencies across the four examinations indicate that Thai-bael fruit extract could potentially inhibit the corrosion reaction of steel electrodes in the acidic solution.

Keywords: Corrosion inhibitors, Carbon steel, Thai-bael fruit.

INTRODUCTION

Due to its excellent mechanical properties such as good toughness and good strength, carbon steel is the most widely used metal in the industries [1]. While the durability of steel is excellent, an inappropriate environment such as air pollutions and moistures may cause premature failures, which are often encountered in petrochemicals, vehicles and machinery applications. Corrosion behaviours of metals and alloys are generally affected by the environment [2]. The environment with pollutants will cause damage to the systems and reduce the machines' lifetime, especially equipment that is in contact with the acid solution. Corrosion of metallic surfaces can be reduced or cont-

rolled by the addition of chemical compounds to the corrodent [3]. This form of corrosion control is termed inhibition. The corrosion inhibitor is one of the best-known methods of corrosion protection and one of the most resorted to in the industry due to its relatively simple implementation and low costs. The corrosion inhibitors will reduce the rate of either anodic oxidation or cathodic reduction or both processes [4]. Commonly, inhibitors are classified into two groups: inorganic inhibitor and organic inhibitors [5]. The inorganic inhibitors may have either cathodic or anodic actions. The mechanism of anodic inhibitors (also called passivation inhibitors) involves either the direct chemical retardation of anode reactions or the support of the passivation reaction of the metal surface. On the other

hand, the cathodic corrosion inhibitors prevent the occurrence of cathodic reactions of the metals. These inhibitors have metal ions capable of undergoing cathodic reactions due to their alkalinity and consequently producing insoluble compounds that precipitate selectively on cathodic sites. Deposited over the metal surface in the form of a compact and adherent film, the compound restricts the diffusion of reducible species. As a result, the covered metal surface possesses a higher impedance and a lower degree of mobility of both reducible species and oxygen ions leading to the overall reduction electrons conductivity of the surface.

The reduction of corrosion rates is mainly due to one or a combination of the following fundamental chemistry [6,7]; (i) adsorption of ions/molecules onto a metal surface, (ii) the increase or decrease in the anodic and/or cathodic reaction, (iii) the decrease in the diffusion rate for reactants to the surface of the metal, and (iv) the decrease in the electrical resistance of metal surface. For example, the inhibitor may be chemically adsorbed (so-called chemisorption) on the surface of the metal and forms a protective thin film. The inhibitor may lead to a formation of an oxide film covering the base metals or reacts with a potential corrosive component presented in aqueous media resulting in a metal complex and depleting the overall bare ion contents in the electrolyte.

In industry-scale applications, inhibitors that could be conveniently prepared and possess *in situ* advantages during service are often utilized. Several factors, including cost, availability and environmental safety, are key imperatives in choosing an inhibitor. In this regard, the organic inhibitors have apparent advantages over inorganic inhibitors such as their non-toxicity and natural abundance [5]. In addition to their inexpensiveness, ready availability and renewability, the organic inhibitors from plant extracts are environmentally friendly and ecologically acceptable. Extracts from a number of the plants have been investigated as corrosion inhibitors in the acid medium [8,9]. Plant extracts have, therefore, been the focus of intense research on corrosion inhibitors for some decades [10]. The organic inhibitors or green corrosion inhibitors can form a protective film of adsorbed molecules on the metal surface, which provides a barrier to the dissolution of metals in electrolyte. One of the key properties of organic inhibitors is their high degree of solubility and dispersibility in the medium surrounding the metals [8-11]. Since the covered metal surface is proportional to the inhibitor concentration, the concentration of the inhibitor in the medium is critical. Recently, organic inhibitors have been extracted from plants or fruits such as Khillah seeds [6], fig leaves [6], aloe vera [8], pineapple, [11], African bush pepper (*Piper guinensis*) [12], papaya [13], parsley (*Petroselium sativum*) [14], *Allium ampeloprasum* [15], ginger [16], onion juice [17], *Gliricidia sepium* leaves [18], anise [19], peach juice [3], red pepper seed oil [20], *etc*.

The organic inhibitors are generally consist of various heteroatoms such as O, N, S and P, which are found to have high Lewis basicity and electron density and thus act as a corrosion inhibitor. The inhibition efficiency should follow the sequence O < N < S < P [21]. These heteroatoms act as active centers for the process of adsorption on the metal surface. Most

organic inhibitors adsorbed on the metal surface by displacing water molecules on the surface and forming a compact barrier. The availability of non-bonded (lone pair) and *p*-electrons in inhibitor molecules facilitates the electron transfer from the inhibitor to the metal. The use of organic compounds containing oxygen, sulfur and nitrogen to reduce corrosion attack on steel has been studied to some extent in literature [22], though not exclusively. Moreover, natural compounds, also known as green corrosion inhibitors, have been extensively used to protect carbon steel materials.

Thai-bael fruit (*Aegle marmelos* L. Correa) is a tropical fruit native in Thailand. The general cultivars known in Thailand are local "Matoom" (Fig. 1) [23,24]. It is commonly found growing in many regions, especially the lower north and central part of Thailand. Among various kinds of fruits, Thai-bael fruit is very rich in vitamins, amino acids and minerals [25]. The bael fruit contains many functional and bioactive compounds such as carotenoids, phenolics, alkaloids and flavonoids [24,26]. Due to its relatively high phenolic content [23], Thai-bael fruit extract could be a good candidate for using in corrosion prevention. To the best of our knowledge, the applicability of Thai-bael fruit extract as corrosion inhibitors of steels has not been explored yet. This work is aimed to systematically study the corrosion-prevention efficiency of Thai-bael fruit extract in acidic HCl solutions.

Fig. 1. Physical appearance of "Matoom" or Thai-bael fruit

EXPERIMENTAL

Steel specimens: Cleaning of the steel samples was carried out using a rough silicon carbide abrasive paper with the number 240, 320, 500, 800, 1000, and 1200, sequentially. The samples were degreased with acetone, rinsed in distilled water, dried in the air, and embedded in PVC holder by epoxy resin. The preparation left a fresh surface area of 1 cm × 1 cm for electrochemical measurements. An X-ray fluorescence (XRF) analysis showed the alloying contents of 0.03 wt% Cr, 0.28 wt% Mn, 0.08 wt% Ni, 0.16 wt% Cu and 99.46 wt% Fe. The XRF instruments used was HORIBA ScientificXGT-5200.

Preparation of plant extract: The dried Thai-bael fruit (*Aegle marmelos*) with the mass of 30 g was boiled in 1000 mL of the deionized water to extract the active ingredient from the fruit. During the extraction process, the mixture was kept

stirring at the speed of 250 rpm for 60 min. The mixture was filtered and adjusted the volume to precisely 1000 mL using a volumetric flask to obtain the stock solution. In order to study the effect of the concentration of the Thai-bael fruit extract on the corrosion behaviour of hot roll steel in HCl medium, a series of the solution has been prepared. Three solutions with the total volume of 500 mL have been used: (i) 1 M HCl without Thai-bael fruit extract, (ii) 1 M HCl solution with 62.5 mL of stock solution of extraction (HCl/TB62.5), and (iii) 1 M HCl solution with 125 mL of stock solution of extraction (HCl/TB125).

FTIR spectroscopy: FTIR characterization was carried out to determine the main functional groups of Thai-bael fruit using a BRUKER Alpha-E spectrometer. A pellet of the sample was obtained by uniaxially pressing the mixture of ground Thai-bael fruit powder and KBr. The FTIR spectrum was recorded in the range from 4000-375 cm^{-1}.

Electrochemical measurement: The experimental electrochemical data was collected and analyzed by the electrochemical software NOVA ver. 1.1 Potentiostat/Galvanistat Autolab PGSTAT 302N. The polarization curves were scanned from -0.54 V to -0.33 V with respect to the open circuit potential at a scan rate of 1 mV s^{-1}. The linear Tafel segments of anodic and cathodic curves were extrapolated to the corrosion potential (E_{corr}) to obtain the corrosion current densities (I_{corr}). Corrosion inhibition was investigated by a potentiodynamic polarization method and their results were compared. The standard silver-silver chloride (Ag/AgCl) and the platinum electrodes were used as a reference and an auxiliary electrode, respectively.

Furthermore, the electrochemical impedance spectroscopy (EIS) measurements were performed using the AC signals with an amplitude of 10 mV. The frequency ranges were set to be 1 MHz to 100 MHz. The samples were equilibrated in the tested solutions for 30 min prior to measurements. The electrical equivalent circuit was constructed from the corresponding EIS spectrum using the fitting functions in NOVA 1.1 software.

Surface microscopy: The surface of carbon steel was analyzed by using an optical microscope modeled Lica DM2700M with 20 times magnification. The images were taken after the sample immersion in acidic solutions up to 4 h. The samples were thoroughly washed with distilled water and dried at room temperature prior to imaging. Qualitative comparisons of the corroded surfaces treated with various concentrations of Thai-bael fruit extract were recorded.

X-Ray absorption near edge structure (XANES): XANES of the carbon steels at different stages was studied by probing the Fe K-edge using fluorescence mode at Beamline 1.1W Multiple X-ray Techniques, Synchrotron Light Research Institute (Public Organization), Thailand. Self-absorption correction was performed prior to the linear combination fitting.

RESULTS AND DISCUSSION

FTIR characterization: The FTIR spectrum is displayed in Fig. 2. An absorption band at 3374 cm^{-1} accounts for the O-H stretch of a phenol group. The medium peak at 2928 cm^{-1} corresponds to the C-H stretching in organic compounds. while the peak at 1603 cm^{-1} is attributed to the C=C stretching vibration of an aromatic ring, while the peak at 1430 cm^{-1} corresponding to the O-H bending of polyphenol and the peak at 1074 cm^{-1} represents C-O stretching of the polyphenol. The small peaks between 900 and 500 cm^{-1} are from aromatic C–H out of plane bending due to substitutions in different positions of the aromatic ring. From all peak responses, it can be concluded that Thai-beal consists of high contents of aromatic rings and phenolics [27].
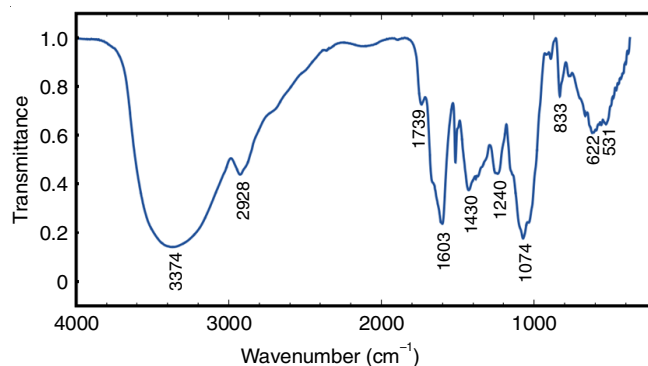

Fig. 2. FTIR spectrum of Thai-bael fruit

Electrochemical measurements: The polarization measurements give information regarding about the kinetics of the corrosion reactions [28]. The polarization curves of electrochemical reactions on carbon steel in 1.0 M HCl solutions in the absence and presence of Thai-beal fruit extract are shown in Fig. 3. From the potentiodynamic polarization curves, it was possible to extrapolate the Tafel-curve fittings to obtain the electrochemical parameters, *i.e.* the corrosion current density (I_{corr}), corrosion potential (E_{corr}), corrosion rate (CR) and anodic and cathodic Tafel coefficient (β_a, β_c). It can be seen from the outcomes (Table-1) that both the cathodic and anodic reactions were affected by the presence of Thai-bael fruit extracts. The decreasing activities in the oxidation/reduction reactions were confirmed by the shift in the β_a and β_c values compared to the inhibition-free solution. Table-1 also shows that the Thai-bael fruit extracts markedly affect both the values of β_a and β_c almost equally. The observation correlates to the decrease in both the overall oxidation and reduction reaction rates on the steel surface at the presence of extract contents, and hence the overall relative reduction in corrosion rates. The addition of the extract contents leads to the significant shifts in the corrosion current density

TABLE-1
POLARIZATION RESISTANCE PARAMETERS OF CARBON STEEL IN (a) BARE 1.0 M HCl, (b) HCl/TB62.5 AND HCl/TB125

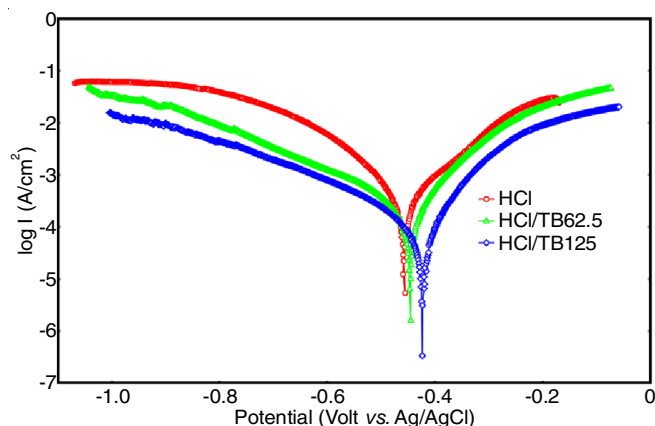| Inhibitor	E_{corr} (mV *vs.* SCE)	I_{corr} (µA cm^{-2})	β_a (mV dec^{-1})	β_c (mV dec^{-1})	CR (mm y^{-1})	IE (%)
HCl (Blank)	-445.8	882.4	116.4	179.0	10.3	–
HCl/TB62.5	-447.5	264.8	107.8	216.6	3.1	70.0
HCl/TB125	-424.6	114.8	94.6	208.4	1.3	87.0

Fig. 3. Polarization curves for carbon steel in 1.0 M HCl in absence and presence of different concentrations of Thai-beal fruit extract

Fig. 4. Nyquist curves of carbon steel in different HCl concentrations containing Thai-bael fruit extract

(I_{corr}) toward a lower value in comparison to the current density of the inhibitor-free solution. This finding indicates that the extract has a mixed-type inhibitor characteristic, where the overall effect is mainly attributed to the reduction of current density in the presence of the extract in 1.0 M HCl [9].

The efficiency of the inhibitors is quantified by the inhibition efficiency (IE%) [20], a measure of the difference in corrosion current densities in the absence (I^{o}_{corr}) and in the presence of the inhibiting species (I^{inh}_{corr}). IE(%) can be represented as follows:

$$IE \ (\%) = \frac{I^{o}_{corr} - I^{inh}_{corr}}{I^{o}_{corr}} \times 100 \qquad (1)$$

where (I^{o}_{corr}) and (I^{inh}_{corr}) are in the unit of (mA cm^{-2}). Furthermore, the corrosion rates were calculated from the expression:

$$\text{Corrosion rate (mm y}^{-1}) = \frac{0.000327 \times I^{inh}_{corr} \times EW}{A \times \rho} \qquad (2)$$

where EW is equivalent to the weight of the metal, A is the surface area of the sample (cm^2) and ρ is the density of metal (g cm^{-3}). The numerical values of inhibition efficiency and the corrosion rates are also reported in Table-1. The numerical outcomes showed that the inhibition efficiency of the tested inhibitor increased with increasing inhibitor concentration, whereas the corrosion rate decreased from approximately 10.3 to 1.3 mm y^{-1} with the increasing amount of inhibitors. The inhibition efficiency obtained reached the value of 87 % for the sample solution of HCl/TB125 (highest concentration of Thai-bael extract investigated). The corrosion current density, in this case, was found to be 114.8 µA cm^{-2}, which is about eight times reduction from the value of inhibition-free solution.

Electrochemical impedance spectroscopy (EIS): The electrochemical impedance results for the mild steel in 1 M HCl solution with the presence and absence of Thai-bael fruit extract are displayed in the form of Nyquist plots in Fig. 4. The results were in line with the observations reported [14]. To understand the relationship between the current and voltage under some periodic perturbation in an impedance experiment, it is best to consider the surface of the working electrode as a charged surface, while the structure of the interface between the electrolyte and the electrode is described as a double layer.
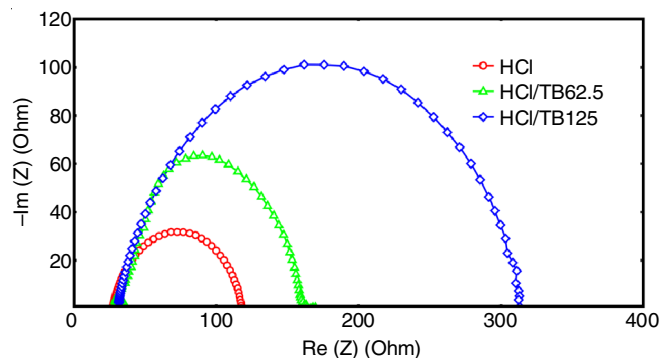
Despite the faradic current discussed in the previous section, there is also a charging current of the double layer. The equivalent circuit model of the electrode charging and the faradic current is given in **Scheme-I**. While there exists numerous equivalent circuit developed to describe this three-electrode system, we will limit our discussion to this simple form. The first circuit element R_s represents the resistance to current flow in the electrolyte. The double layer is simply treated as a capacitor C_{dl} in parallel with an element representing the resistance to charge transfer R_f. The solution resistance R_s is assigned at the high-frequency intercept, while the value transfer resistance R_s + R_f is the low-frequency intercept on the real axis in the Nyquist plot. This equivalent circuit allows us to understand the response of the electrode surface adsorbed with organic molecules derived from Thai-bael fruit extracts. More specifically, how the charging current can affect the corrosion of the working electrode in an acidic solution. A constant phase element (CPE) is often used in place of pure capacitor for the derivations of the ideal dielectric behaviours of double layers. The CPE is a conceptual device that accounts for electrode surface inhomogeneity [29]. The impedance, Z_{CPE} for a rough solid electrode is described by the expression:

$$Z_{CPE} = \frac{1}{Y_o (j\omega)^n} \qquad (3)$$

where Y_o is the proportionality constant, ω is the angular frequency, and n is the CPE exponent that can be used as a measure of the surface roughness/heterogeneity. The double-layer capacitance (C_{dl}) derived from the CPE can be calculated as follows [30]:
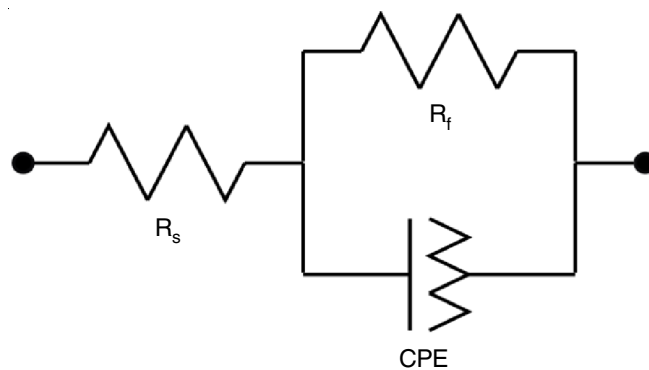
Scheme-I: Equivalent circuit diagram for an EIS measurement

$$C_{dl} = (Y_o R_f^{1-n})^{1/n} \qquad (4)$$

The constant phase elements identify the mechanism of the steel dissolution in the absence and presence of the organic molecules. The ideal capacitor is equivalent to the CPE when $n = 1$. To determine the EIS parameters, the experimental semi-circles were fitted to the theoretical ideal semicircles using the available numerical fitting routines in NOVA 1.1 software. It is possible to extract from this Z-curve the data concerning the R_s, R_f and CPE, as listed in Table-2. An increase in the concentration of Thai-bael fruit extracts results in the increase in the magnitude of R_f, which reaches a maximum value of 380.520 W cm^2 in case of HCl/TB125. The increase in charge-transfer resistance R_f in the presence of the inhibitor with the increase in the inhibitor concentration suggests the formation of a protective layer on the steel, hence inhibition increases. Therefore, as the value of R_f increases, the speeding of corrosion decreases. The addition of the inhibitors also results in the increasing 'n' value indicating the reduction of surface inhomogeneity due to molecular adsorption on the most active adsorption sites on the steel surface [31].

The value of the proportional factor Y_o also changes with the concentration of inhibitors. This noticeable variation in the values of R_f and Y_o is correlated with the magnitude of the displacement of water molecules by organic molecules belonging to the inhibitors on the steel surface. The adsorption of inhibiting chemical species on the steel surface decreases its electrical capacity because they tend to displace the water molecules and other ions initially adsorbed on the surface. The reduction of the capacity with increasing organic chemical species is partly attributed to the formation of protective layer on the steel surface. The thickness of this protective layer increases with the organic inhibitor concentration, *i.e.* the greater the amount of the adsorbed molecules, the greater the in C_{dl}. This trend is in agreement with the Helmholtz model for the electrical double layer [32], which is represented as follows:

$$C_{dl} = \frac{\varepsilon \varepsilon_o}{d} \qquad (5)$$

where d is the thickness of the protective layer, ε is the dielectric constant of the protective layer and ε_o is the permittivity of free space. It should also be noted that despite the enhanced displacement of water molecules, the decrease in C_{dl} values can be very well ascribed to the decrement in the local dielectric constant. In total, the general reduction in double-layer capacitance with the addition of Thai-bael extracts indicates that the investigated organic inhibitors are effectively adsorbed on the steel surface at both anodic and cathodic sites [33].

The variation in both R_f and Y_o can be correlated with the decreases in the active sites for chemical reduction reactions,

hence resulting in the delayed corrosion process. The inhibition efficiency (η) can be calculated from R_f as follows:

$$\eta \, (\%) = \frac{R_f^{inh} - R_f^o}{R_f^{inh}} \times 100 \qquad (6)$$

where R_f^o and R_f^{inh} represent the faradic resistance within the inhibited solution and blank solution, respectively. The data is also shown in Table-2.

Surface imaging: The surface morphology of carbon steel surfaces unexposed and exposed to the HCl solutions in the absence and presence of Thai-bael fruit extract were examined using an optical microscope. A close examination of the images in Fig. 5 revealed that the carbon steel specimens exhibited a very rough surface in absence of the inhibitor (the first columns of Fig. 5). In the third and fourth columns, surfaces of the samples immersed in the inhibitor solutions appeared comparatively smoother, where the number of black spots and visible defects were relatively lower than those of the samples immersed in the pure acidic solution. This confirms the corrosion inhibiting reactivity of Thai-bael fruit extract in the form of an anti-corrosion film that withstands 0-4 h of exposure to the acidic solution.

X-ray absorption near edge structure (XANES): In order to identify the effect of Thai-Bael fruit extract (TB) for inhibiting the corrosion of carbon steels, X-ray absorption near edge structure (XANES) probing at Fe K-edge of the carbon steels at different stages of the corrosion inhibitor study were investigated. According to XANES spectra (Fig. 6), carbon steel prior to the corrosion inhibitor test (black plot) exhibit the similar XANES fingerprint as the standard Fe(0) foil (green plot) indicating the oxidation state of zero of Fe species in the carbon steel prior to the reaction. After performing the electrochemical linear polarization measurements (Fig. 6a), the carbon steel soaking in HCl solution without TB (red plot) showed a higher fraction of the spectral shift towards the higher energy with respect to one soaking in HCl solution with the presence of TB extraction (blue plot). This observation indicates the higher fraction of iron oxides in the case of soaking the steel in HCl solution without TB extraction. A similar trend was also observed in the case of electrochemical impedance spectroscopic measurement (EIS) as shown in Fig. 6b. Linear combination fitting (LCF) of the observed XANES spectra (Table-3) shows the detailed fraction of iron oxides after the corrosion inhibitor test *via* an electrochemical reaction. These observations indicate the performance of Thai-Bael fruit extract (TB) for preventing corrosion in carbon steels.

Conclusion

This work provides a proof of concepts for the corrosion inhibition of carbon steel in the acid medium using Thai-bael

TABLE-2 IMPEDANCE ELEMENTS DERIVED FROM SPECTRA RECORDED FOR CARBON STEEL IN 1 M HCl SOLUTION COMPARED WITH HCl WITH DILUTED THAI-BEAL EXTRACT					
Inhibitor	R_f (Ω cm^2)	10^6Y (Ω^{-1} s^n cm^{-2})	n	C_{dl} (μF cm^{-2})	η (%)
HCl	87.603	345	0.865	199.8	–
HCl/TB62.5	242.800	937	0.356	64.4	63.91
HCl/TB125	380.520	379	0.521	63.9	76.98

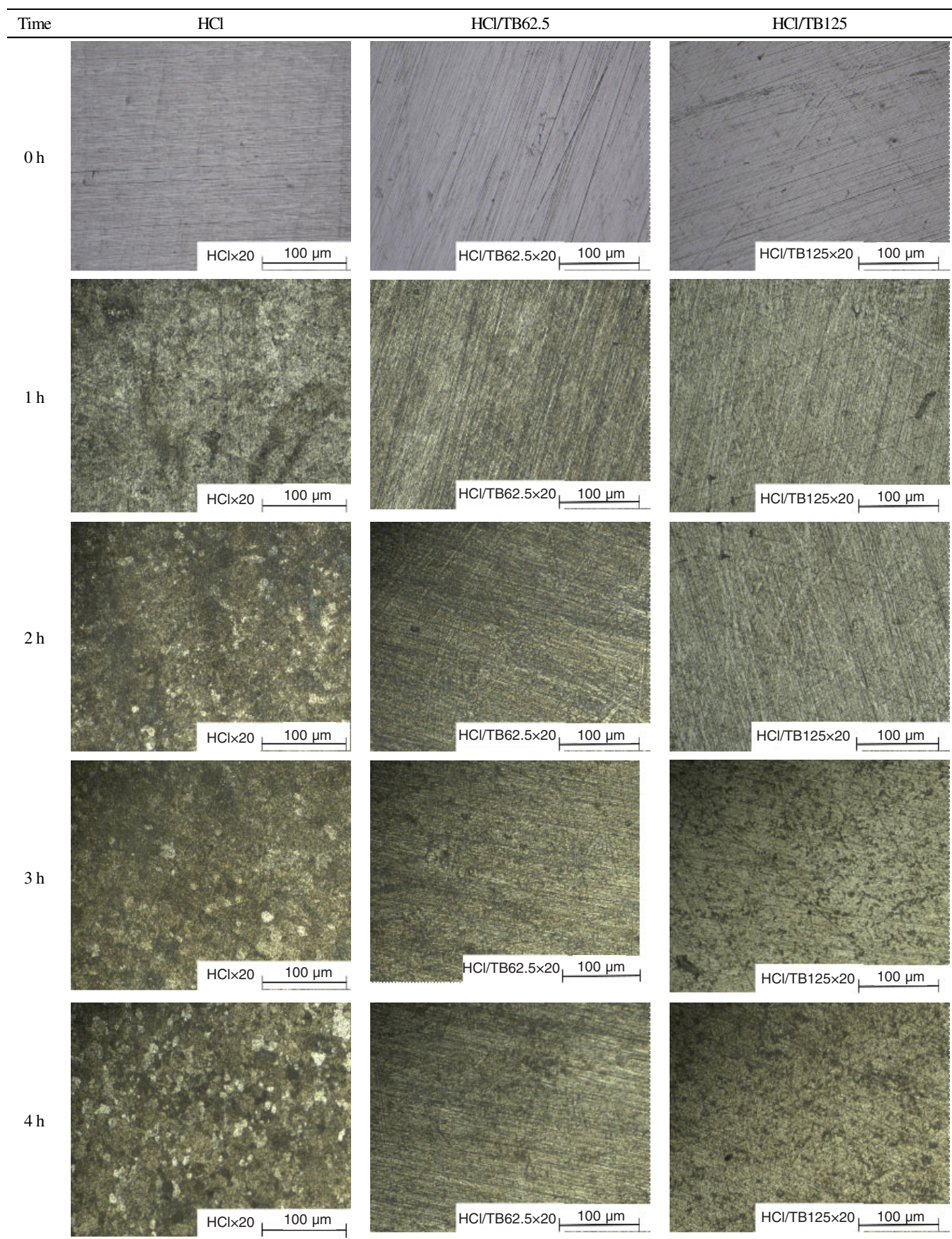| Time	HCl	HCl/TB62.5	HCl/TB125

Fig. 5. Micrographs of carbon steel as observed under an optical microscope after soaking in HCl solutions with and without the inhibitor extract at 20X
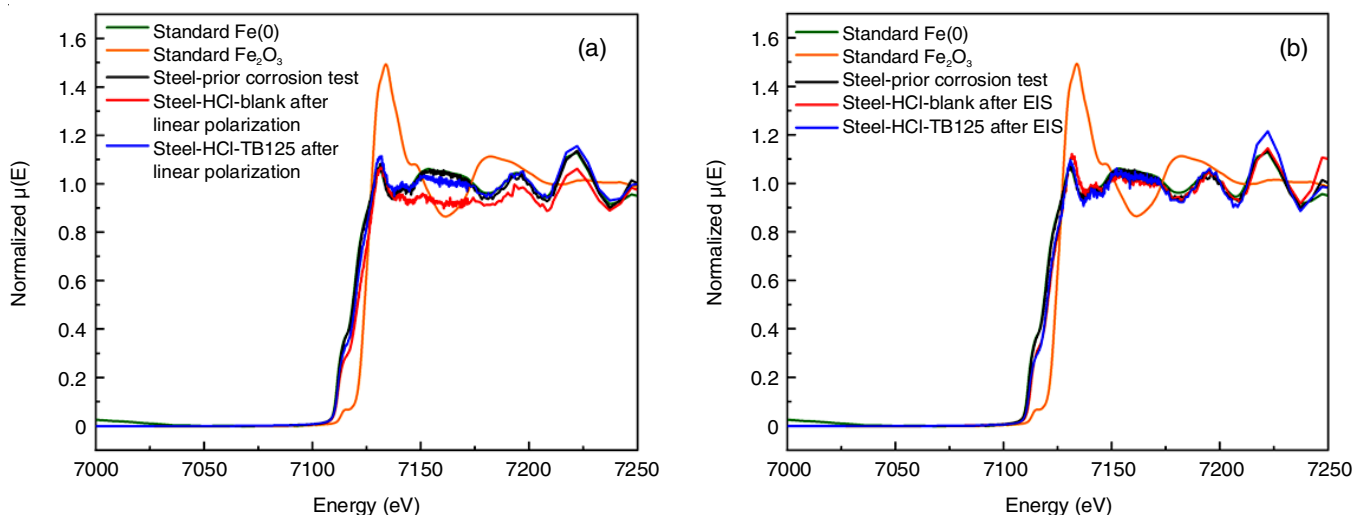
Fig. 6. X-ray absorption near edge structure (XANES) probing at Fe K-edge of the carbon steels at different stages of the corrosion inhibitor study *via* (a) electrochemical linear polarization measurements and (b) electrochemical impedance spectroscopic measurement (EIS)

TABLE-3
LINEAR COMBINATION FITTING (LCF) OF THE CARBON STEELS AT DIFFERENT STAGES OF THE CORROSION
INHIBITOR STUDY SHOWING THE COMPOSITION OF IRON(0) AND IRON OXIDES AFTER THE CORROSION TEST

Conditions	Fraction of compositions (%)	
	Fe(0)	Fe(III)
Steel-prior to corrosion test	98.3	1.70
Steel-HCl-blank-after linear polarization measurement	78.2	21.8
Steel-HCl-TB125-after linear polarization measurement	87.2	12.8
Steel-HCl-blank-after electrochemical impedance spectroscopic measurement	87.6	12.4
Steel-HCl-TB125-after electrochemical impedance spectroscopic measurement	89.4	10.6

fruit extract as a green corrosion inhibitor. Results from the potentiodynamic polarization measurements suggested that the inhibiting character of Thai-bael fruit extract was a mixed-type inhibitor where the reactivity on both the cathodic and anodic branches were affected by the presence of the inhibitors. At the highest concentration of Thai-bael extract in the acidic medium investigated, the smallest corrosion rate, calculated from the results of potentiodynamic poloarization measurements, was about 1.3 mm y⁻¹, as compared to 10.3 mm y⁻¹ in the case of no added inhibitor. Under the EIS investigation, Faradic resistance (charge-transfer resistance) increased with the addition of the organic inhibitors indicating that a protective layer has been formed. The molecules of extracts were adsorbed as seen from the reduction in the double-layer capacitance, signifying that the organic molecules were effectively adsorbed onto the metal surface. The EIS also demonstrated that the inhibition efficiency of mild steel in 1.0 M HCl increased with a higher concentration of Thai-bael fruit extract. In line with results from the electro-chemical techniques, the surface morphology revealed that the samples immersed in liquid solutions of inhibiting compounds and HCl showed less roughness and visible defects compared to the ones immersed in a pure HCl solution. X-ray absorption near edge structure results showed that the Fe K-edge positions of the samples immersed in the HCl solution without the inhibitor closer to that of Fe_2O_3 standard than the Fe K-edge positions of the samples soaked with HCl solutions and Thai-bael fruit extract. Moreover, the linear combination fitting of

XANES spectra showed that Fe_2O_3 content decreased from 21.8% to 12.8% in case of the sample from the linear polarization measurement and from 12.4% to 10.6% in case of the sample from the EIS measurement. All aforementioned findings suggested the that the compounds derived from Thai-bael fruit are effective green corrosion inhibitors for carbon steel.

REFERENCES

1. C.C. Chama, *Int. J. Eng. Res. Africa*, **12**, 25 (2014);
    https://doi.org/10.4028/www.scientific.net/JERA.12.25
2. M. Natesan, S. Selvaraj, T. Manickam and G. Venkatachari, *Sci. Technol. Adv. Mater.*, **9**, 045002 (2008);
    https://doi.org/10.1088/1468-6996/9/4/045002

3. A.S. Yaro, A.A. Khadom and H.F. Ibraheem, *Anti-Corros. Methods Mater.*, **58**, 116 (2011);
https://doi.org/10.1108/00035591111130497

4. S. Lyon, ed.: D. Fron, Overview of Corrosion Engineering, Science and Technology, In: Nuclear Corrosion Science and Engineering, Woodhead Publishing Series in Energy: Number 22, pp. 1-30 (2012).

5. C.G. Dariva and A.F. Galio, in ed.: E. Hart, Developments in Corrosion Protection, In: Corrosion Inhibitors-Principles, Mechanisms and Applications, Nova Science Publishers Inc., p. 122 (2014).

6. B.E.A. Rani and B.B.J. Basu, *Int. J. Corros.*, **2012**, 1 (2012);
https://doi.org/10.1155/2012/380217

7. C. Verma, M.A. Quraishi, M. Makowska-Janusik, L.O. Olasunkanmi, K. Kluza and E.E. Ebenso, *Sci. Rep.*, **7**, 44432 (2017);
https://doi.org/10.1038/srep44432

8. O.K. Abiola and A.O. James, *Corros. Sci.*, **52**, 661 (2010);
https://doi.org/10.1016/j.corsci.2009.10.026

9. P.B. Raja and M.G. Sethuraman, *Mater. Lett.*, **62**, 113 (2008);
https://doi.org/10.1016/j.matlet.2007.04.079

10. J.C.O.C. Okere, *Food Technol.*, **4**, 61 (2013).

11. M. Mobin, M. Basik and J. Aslam, *Measurement*, **134**, 595 (2019);
https://doi.org/10.1016/j.measurement.2018.11.003

12. A. Singh, I. Ahamad and M.A. Quraishi, *Arab. J. Chem.*, **9**, S1584 (2016);
https://doi.org/10.1016/j.arabjc.2012.04.029

13. N. Chaubey, V.K. Singh and M.A. Quraishi, *Ain Shams Eng. J.*, **9**, 1131 (2018);
https://doi.org/10.1016/j.asej.2016.04.010

14. M. Benarioua, A. Mihi, N. Bouzeghaia and M. Naoun, *Egypt. J. Petrol.*, **28**, 155 (2019);
https://doi.org/10.1016/j.ejpe.2019.01.001

15. H. Hussein, *Int. J. Mechan. Eng. Technol.*, **6**, 34 (2015).

16. A. Fidrusli, Suryanto and M. Mahmood, *IOP Conf. Series Mater. Sci. Eng.*, **290**, 012087 (2018);
https://doi.org/10.1088/1757-899X/290/1/012087

17. A.Y. El-Etre, *Bull. Electrochem.*, **22**, 75 (2006).

18. A.E. Okoronkwo, S.J. Olusegun and O. Olaniran, *Afr. Corros. J.*, **1**, 30 (2015).

19. A. Fouda, G.Y. Elewady, K. Shalabi and S. Habouba, *Int. J. Adv. Res.*, **2**, 817 (2014).

20. F. Kurniawan and K.A. Madurani, *Prog. Org. Coat.*, **88**, 256 (2015);
https://doi.org/10.1016/j.porgcoat.2015.07.010

21. A. Cojocaru, I. Maior, D.I. Vaireanu, C. Lingvay, I. Lingvay, S. Caprarescu And G.E. Badea, *J. Sustainable Energy*, **1**, 64 (2010).

22. M.H.O. Ahmed, A.A. Al-Amiery, Y.K. Al-Majedy, A.A.H. Kadhum, A.B. Mohamad and T.S. Gaaz, *Results in Physics*, **8**, 728 (2018);
https://doi.org/10.1016/j.rinp.2017.12.039

23. S.A. Charoensiddhi and P. Anprung, *Int. Food Res. J.*, **15**, 287 (2008).

24. S.K. Roy and S. Saran, ed.: E.M. Yahia, Bael *(Aegle marmelos* (L.) Corr. Serr.*)*, In: Postharvest Biology and Technology of Tropical and Subtropical Fruits, Extension Systems Internationa: USA, pp. 186-215 (2011).

25. N.K. Gupta, K.K. Misra, O. Singh and R. Rai, *Progress. Hortic.*, **48**, 116 (2016);
https://doi.org/10.5958/2249-5258.2016.00023.3

26. R. Pati and M. Muthukumar, eds.: S. Jain and S.D. Gupta, Genetic Transformation of Bael *(Aegle marmelos* Corr.), In: Biotechnology of Neglected and Underutilized Crops, Springer: Dordrecht, pp. 343-365 (2013).

27. H. Pynam and S.M. Dharmesh, *Biomed. Pharmacother.*, **106**, 98 (2018);
https://doi.org/10.1016/j.biopha.2018.06.053

28. T.F. Fuller and J.N. Harb, Electrochemical Engineering, John Wiley & Sons (2018).

29. M.E. Orazem and B. Tribollet, Electrochemical Impedance Spectroscopy, John Wiley & Sons, edn 2, vol. 48 (2017).

30. M.R.S. Abouzari, F. Berkemeier, G. Schmitz and D. Wilmer, *Solid State Ion.*, **180**, 922 (2009);
https://doi.org/10.1016/j.ssi.2009.04.002

31. M. Outirite, M. Lagrenée, M. Lebrini, M. Traisnel, C. Jama, H. Vezin and F. Bentiss, *Electrochim. Acta*, **55**, 1670 (2010);
https://doi.org/10.1016/j.electacta.2009.10.048

32. A.J. Bard and L.R. Faulkner, Electrochemical Methods Fundamentals and Applications, John Wiley & Sons, Inc., edn 2, vol. 38, p. 850 (2001).

33. Sudheer and M.A. Quraishi, *Ind. Eng. Chem. Res.*, **53**, 2851 (2014);
https://doi.org/10.1021/ie401633y